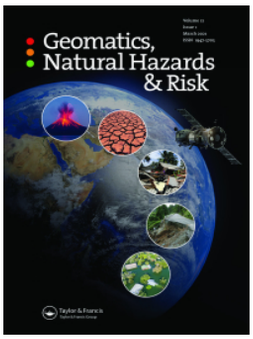

Geomatics, Natural Hazards and Risk

ISSN: (Print) (Online) Journal homepage: https://www.tandfonline.com/loi/tgnh20

Estimation of V_{S30} using shallow depth time-averaged shear wave velocity of Rawalpindi–Islamabad, Pakistan

Muhammad Bilal Adeel, Zubair Ahmed Nizamani, Muhammad Aaqib, Sarfraz Khan, Jawad Ur Rehman, Bikram Bhusal & Duhee Park

To cite this article: Muhammad Bilal Adeel, Zubair Ahmed Nizamani, Muhammad Aaqib, Sarfraz Khan, Jawad Ur Rehman, Bikram Bhusal & Duhee Park (2023) Estimation of V_{S30} using shallow depth time-averaged shear wave velocity of Rawalpindi–Islamabad, Pakistan, Geomatics, Natural Hazards and Risk, 14:1, 1-21, DOI: 10.1080/19475705.2022.2161953

To link to this article: https://doi.org/10.1080/19475705.2022.2161953

Published online: 02 Jan 2023.

GEOMATICS, NATURAL HAZARDS AND RISK
2023, VOL. 14, NO. 1, 1–21
https://doi.org/10.1080/19475705.2022.2161953

Taylor & Francis
Taylor & Francis Group

Estimation of V_{S30} using shallow depth time-averaged shear wave velocity of Rawalpindi–Islamabad, Pakistan

Muhammad Bilal Adeel[a], Zubair Ahmed Nizamani[b], Muhammad Aaqib[c], Sarfraz Khan[d], Jawad Ur Rehman[e], Bikram Bhusal[f] and Duhee Park[e]

[a]Department of Transportation & Geotechnical Engineering, National University of Sciences and Technology, Risalpur, Pakistan; ; [b]Department of Civil Engineering, National University of Sciences and Technology, Quetta, Pakistan; [c]Department of Civil Engineering, National University of Technology, Islamabad, Pakistan; [d]National Centre of Excellence in Geology, University of Peshawar, Peshawar, Pakistan; [e]Department of Civil and Environmental Engineering, Hanyang University, Seoul, Republic of Korea; [f]Department of Civil Engineering, National College Engineering, Lalitpur, Nepal

ABSTRACT

The time-averaged shear wave velocity of top 30 m (V_{S30}) is the most commonly used parameter to classify a site and evaluate its amplification characteristics for the seismic design. The in-situ seismic tests must be performed up to a depth of 30 m for obtaining the shear wave velocity (V_S) profiles to estimate V_{S30}. It is intimated that, in most of the cases, the measured V_S profile does not extend up to 30 m due to numerous reasons including limitation of testing techniques and unfavorable field conditions. Since, the measurements of V_{S30} are unavailable for the majority of Pakistan and the world, the local geology and topographic slope or its combination are used to estimate V_{S30}. However, there is no field-based validation of the estimated V_{S30} is performed in Islamabad–Rawalpindi region, the proxy-based estimation may lead to unrealistic results. To accommodate this, region specific extrapolation methods are developed. This study develops an empirical data-driven function of V_{S30} from shallow V_S profiles by correlating V_{S30} with the time-averaged V_S to depths less than 30 m. In this regard, 85 V_S profiles are used from Rawalpindi-Islamabad region. A comparative analysis of the proposed procedure is carried out with the published methods. It is revealed that V_{S30} predicted by the proposed function results in close matches with the data measured in the western United States. In addition, the results indicate that the local geology and topographic slope proxies may not be acceptable for usage in the region due to their greater uncertainty. Finally, a procedure for extrapolating the V_S profile from available shallow depth measurements up to 30 m is proposed.

ARTICLE HISTORY
Received 10 October 2022
Accepted 19 December 2022

KEYWORDS
Time-averaged shear wave velocity; shallow depth; V_{S30}; empirical function; building code of Pakistan

CONTACT Bikram Bhusal bikram@nce.edu.np

1. Introduction

The shear wave velocity (V_S) of a site represents the dynamic characteristics of a site. It provides the foundation to assess the site amplification factors in quantifying the local site effects due to earthquake shaking using site specific ground response analysis (Kramer 1996). The characteristics of vertically propagated horizontal shear waves from bedrock are significantly influenced by the top 30 m strata (Anderson et al. 1996; Kuo et al. 2011). Therefore, the time-averaged shear wave velocity of the top 30 m (V_{S30}) is widely utilized as a proxy to evaluate the variation of the ground motion as it travels through the soil medium to surface (Boore et al. 1997). V_{S30} is the primary parameter used in various site classification systems (BCP 2007; ICC I 2015). The building code of Pakistan (BCP 2007) is based on the National Earthquake Hazard Reduction Program (NEHRP) provisions (Council BSS 1997) and characterize the sites into five categories listed in Table 1. Furthermore, V_{S30} is commonly used in the development of site amplification models (Aaqib et al. 2021; Chiou and Youngs 2014; Seyhan and Stewart 2014; Harmon et al. 2019; Tran et al. 2021) which are subsequently employed in the ground motion prediction equations (GMPEs) (Campbell and Bozorgnia 2008) and their ranking and testing for seismic hazard analysis (Bindi et al. 2006; Nizamani and Park 2021) and also for the site-specific response analyses (Nguyen et al. 2020; Tran et al. 2021; Bhusal et al. 2022; Gaha et al. 2022) and microzonation studies (Thompson et al. 2010; Khan and Khan 2018).

A considerable challenge lies in the measurement of V_S profiles for regions where the economic conditions are constrained, such as Pakistan (Sadiq et al. 2021). The availability of measured V_S profiles up to 30 m is important for characterization of the site to perform a seismic design. However, in most of cases, the profile does not extend up to 30 m due to numerous circumstances including unfavorable field conditions and limitation of the testing equipment (Sun et al. 2005; Sun 2015; Aaqib et al. 2020; 2022). In such cases, the V_S profiles are empirically derived from the standard penetration test (SPT) data (Manandhar et al. 2018; Adeel et al. 2020; Adeel et al. 2022). Even the availability of the SPT data up to 30 m is not always warranted (Lodi et al. 2015).

Recently, a number of studies have been carried out to estimate V_{S30} based on various proxy methods such as topography, geology, and geomorphology. Wald and Allen (2007) and Allen and Wald (2009) proposed a procedure to compute V_{S30} based on the topography of the region in the absence of geological and geotechnical site information. Estimating V_{S30} as a proxy from horizontal to vertical spectral ratio (HVSR) has also been

Table 1. Site classification system in Building code of Pakistan (BCP 2007).

		Average properties of top 30 m soil profile		
Site	Description	Shear wave velocity, V_{S30} (m/s)	Standard penetration test, blow count, N	Undrained shear strength, s_u (kPa)
S_A	Hard rock	>1500	–	–
S_B	Rock	750–1500	–	–
S_C	Very dense soil/Soft rock	350–750	>50	>100
S_D	Stiff soil	175–350	15–50	50–100
S_E	Soft soil	<175	<15	<50
S_F	Soil require site-specific evaluation			

proposed and widely used (Pokhrel et al. 2019; Yaghmaei-Sabegh and Rupakhety 2020). Wills and his colleagues (Wills et al. 2000; Wills and Clahan 2006; Wills et al. 2015) utilized geological units to estimate V_{S30} values from the geologic map in California, United States. Xie et al. (2016) employed surface geology and Quaternary depth to the Beijing Plain to develop a V_{S30} prediction model. Li et al. (2019) took geologic age and grain size into account while constructing a China site categorization map. Recently, Shafique et al. (2018) developed seismic site characterization map and classification maps by correlating instrument based V_{S30} measurements with geological units for northern Pakistan. Given the lack of *in situ* V_{S30} observations, these regional-scale proxies-based V_{S30} calculations can cause large amount of uncertainties. Moreover, due to site characteristics and high risk of earthquake in Islamabad–Rawalpindi region, a more precise V_{S30} calculation method is needed to evaluate seismic site conditions.

In cases where the measurements do not extend up to 30 m, V_{S30} has been empirically correlated with shallower time-averaged shear wave velocities and also to extrapolate V_S profile up to 30 m. Boore (2004; hereafter referred to as B04) proposed two methods to evaluate V_{S30} from shallow V_S profiles. A total of 135 boreholes from California were utilized for this purpose. The first method assumed a constant velocity from the shallowest depth of available V_S profile to 30 m whereas in the second method, the correlation between V_{S30} and mean V_S to the shallower depths was proposed, defined as follows:

$$\log\ V_{S30} = a\ +\ b \log V_{SZ} \tag{1}$$

where V_{SZ} represents the time-averaged V_S from surface to the shallow depth (z) whereas a and b are depth dependent regression coefficients. Cadet and Duval (2009) used Eq. (1) proposed by B04 and investigated the correlations between V_{S30} and average V_S to five representative depths of 5, 10, 20, 50 and 100 m. A total of 504 V_S profiles from Japan and 22 V_S profiles from Europe were utilized. Boore et al. (2011) implemented Eq. (1) to investigate the relationship between V_{S30} and averaged V_S to five representative depths of 5, 10, 15 and 20 m. A total of 638 V_S profiles from KiK-net database of Japan, 228 V_S profiles from Turkey, 135 V_S profiles from California and 21 V_S profiles from Europe were utilized. They concluded that the empirical correlation of B04 may not be appropriate for the Japanese sites, which led to the modification of Eq. (1) for that region. Sun (2015; hereafter referred to as S15) used 72 V_S profiles from Korea to propose a method for calculating V_{S30} from shallow V_S profiles. V_{S30} was extrapolated from shallow V_S profiles by correlating it with the mean V_S up to the five representative shallow depths, employing the following function:

$$V_{S30} = \frac{V_{SZ}}{0.2143\ z^{0.4529}} \tag{2}$$

Furthermore, a function for extrapolating the V_S from shallow depths to 30 m was also proposed, defined as follows

$$V_S = -0.403\ z_c{}^2 + 30.875\ z_c - V_S\ (z_c) \tag{3}$$

where z_c is the depth at which V_S is calculated and V_S (z_c) is defined as follows

$$V_S(z_c) = -0.403\ z_{c(\text{cut off})}{}^2 + 30.875\ z_{c(\text{cut off})} - V_{S\ (\text{cut off})} \tag{4}$$

where, $z_{c(\text{cut off})}$ and $V_{s(\text{cut off})}$ indicates the depth of the deepest V_s available and V_s at that depth, respectively. Mahmood et al. (2016) performed 1D site response analysis of collapsed Margalla Tower in Islamabad during 2005 Kashmir Earthquake. They used SPT measurements of the site and established V_S profile using the Lee (1990) correlation. The site was characterized as Sc according to BCP (2007). A total of four ground motions were used from Pacific Earthquake Engineering Research Center (PEER) database with magnitude ranging 7–7.6 with closest distance. It was concluded that the amplification factors using all the four-input ground motions were amplified up to 2.25, overestimating the design values recommended by BCP (2007). Lodi et al. (2015; hereafter referred to as LEA15) employed a method similar to B04 to compute V_{S30} from shallow velocity profiles. A total of 140 SPT profiles from the Karachi region of Pakistan with $z > 30$ m were utilized. However, the V_S profiles were estimated from SPT profiles using the empirical correlations. It was reported that the use of SPT profiles to calculate V_S adds uncertainty in the conversion (Aaqib et al. 2018).

Wang and Wang (2015; hereafter referred to as WW15) used a suite of dataset comprising of 135 boreholes from California and 594 boreholes from KiK-net in Japan to develop and investigate the reliability of proposed method to calculate V_{S30} from known shallow depth time-averaged shear wave velocities at two depths. A simple extrapolation/interpolation method was proposed to calculate Vs_z at a depth. If z is set to 30 m, the equation becomes as follows:

$$\log\ V_{S30} = \log\ V_{S(z_2)} + \frac{\log 30 - \log z_2}{\log z_2 - \log z_1}\ \left[\log V_{S(z_2)} - \log V_{S(z_1)}\right] \tag{5}$$

where $V_{s(z1)}$ and $V_{s(z2)}$ are time-averaged shear wave velocities at depths z_1 and z_2, respectively. The limitation of this study is that the whole V_S profile is required.

Zhou et al. (2021; hereafter referred to as ZEA21) compiled a dataset of 8831 boreholes in China and evaluated several published models based on the dataset to develop a parametric model for estimating V_{S30} from shallow borehole profile. Similar to WW15, ZEA21 also has the limitation that if the V_S profile is not available, the model becomes inapplicable. Midorikawa and Nogi (2015) was one of the evaluated models by ZEA21 and was used to develop the M-Pt model in their study. The functional form used to develop M-Pt model is as follows:

$$V_{S30} = \frac{30}{\left(\frac{z}{VSz}\right) + \left(\frac{30-z}{VSz30}\right)} \tag{6}$$

where, V_{Sz30} is defined as follows:

$$\log V_{Sz30} = a\ +\ b \log V_{SZ} \tag{7}$$

where a and b are model specific regression coefficients.

A specific interest of this study is the Rawalpindi–Islamabad region, located in the northern part of Pakistan. The northern part poses a significant threat to the seismic hazard because it lies in the vicinity of the seismically active fault Main Boundary Thrust (MBT). Rapid economic and infrastructure growths has taken place in the capital area of Pakistan, further increasing the societal risk to a devastating earthquake such as the 2005 Kashmir event (moment magnitude = 7.6). This earthquake caused more than 80,000 casualties and 100,000 injuries, while leaving 2.8 million people homeless (Durrani et al. 2005). Some severe repercussions include the collapse of multistory Margalla Towers, Islamabad, located over 80 km from the epicenter. The Building Code of Pakistan (BCP 2007) classifies capital region as Zone 2B, for which the peak ground acceleration (PGA) ranges from 0.19 to 0.26 g. The subsurface geology of the northern part of Pakistan is quite different than southern part of the country (Khan and Khan 2018). As a result, the model proposed by LEA15 cannot be directly used for site characterization except for the host region.

This study proposes a method to predict V_{S30} from shallow V_S profiles in the Rawalpindi–Islamabad region. A total of 85 V_S profiles were collected from Rawalpindi–Islamabad. The least squares regression is performed to correlate V_{S30} with the mean V_S at five representative shallow depths. Additionally, a method for extrapolating the Vs profile up to 30 m from shallow V_S profiles in the study region is also developed. Furthermore, a comparative study is conducted with the selected published procedures to assess the effectiveness of the proposed method.

2. Local geology and site profiles

The city of Islamabad is the capital of Pakistan and is located at 33.43° N and 73.04° E, at the brink of Potwar plateau. Rawalpindi is a twin city linked to the capital. The Islamabad region is a section of the sub-Himalayas as reported by Gansser (1964), defined by the Potwar plateau and salt ranges in Pakistan (Gee and Gee 1989). The Rawalpindi–Islamabad metropolitan area occupies one of the chief Himalayan boundary faults (Khan and Khan 2018). Quaternary sediments dominate most of the region. The area consists of the gravelly deposits which are exhibited all along the Margalla hills (Khan et al. 2020). The seismic hazards in the Rawalpindi–Islamabad metropolitan area are substantially connected with various faults in the vicinity of the region, consisting of the Main Boundary Thrust (MBT), the Panjal, Margalla, Hazara, Murree, Jhelum and Mansehra faults (Monalisa et al. 2007; Yong et al. 2008).

In this study, the V_S profiles documented in Khan et al. (2020) at 85 locations covering the Rawalpindi-Islamabad region are used. The testing procedures are explained in Khan et al. (2020). The testing locations and site characteristics are shown in Table 2. Figure 1 presents the location of sites where tests were performed. It also shows that the locations of bore holes cover the entire study area. Figure 2 shows V_{S30} of each soil profile. The sites classified according to BCP (2007) are also presented. A total of 36 profiles falls under site class C, 47 are classified as site class D whereas 2 sites are classified as site class E. V_{S30} of the profiles is calculated as follows

Table 2. Testing locations and characteristics of sites (modified after Khan et al. 2020).

Site No.	Longitude (°)	Latitude (°)	Depth, H (m)	V_{S30} (m/s)	Site class, BCP (2007)
1	72.94	33.63	39.2	310.853	D
2	73.11	33.74	37.6	453.417	C
3	73.04	33.69	81.2	283.482	D
4	73.24	33.78	5.5	389.012	C
5	73.2	33.74	4.9	505.714	C
6	73.16	33.64	31.1	369.71	C
7	73.06	33.74	1.8	328.939	D
8	73.16	33.52	108.2	147.69	E
9	73.09	33.55	24.5	154.604	E
10	73.18	33.53	79.5	249.503	D
11	73.24	33.55	20.7	477.348	C
12	72.97	33.7	4.2	418.984	C
13	73.04	33.73	111.1	270.265	D
14	73.1	33.72	13	325.879	D
15	72.99	33.68	40.9	241.569	D
16	73	33.68	65.1	243.545	D
17	72.92	33.64	20.7	269.018	D
18	73.08	33.73	111.1	271.544	D
19	73.04	33.71	111.1	286.366	D
20	73.03	33.72	111.1	266.949	D
21	73.03	33.71	35.7	248.875	D
22	73.04	33.73	1.4	381.753	C
23	73.08	33.68	19.6	416.804	C
24	72.99	33.67	135.5	248.692	D
25	72.96	33.65	8.2	340.722	D
26	72.96	33.65	111.1	261.602	D
27	72.92	33.63	38.1	238.472	D
28	72.92	33.63	27	256.557	D
29	72.92	33.64	13.3	295.902	D
30	72.92	33.63	21.6	266.268	D
31	73.08	33.7	8.7	370.289	C
32	73.05	33.71	40.9	224.944	D
33	73.03	33.69	109.1	284.559	D
34	73.03	33.68	111.1	269.425	D
35	73.03	33.69	77.6	398.424	C
36	73.16	33.67	55.1	210.427	D
37	73.15	33.6	19.6	254.657	D
38	73.11	33.56	47.8	413.06	C
39	73.01	33.66	21.6	254.363	D
40	72.99	33.65	3.9	420.502	C
41	73.05	33.67	23	344.635	D
42	73.04	33.66	20.7	270.339	D
43	73.03	33.64	16.7	276.894	D
44	73.05	33.66	111.1	265.001	D
45	73.23	33.57	5	366.8	C
46	73.15	33.73	135.5	274.184	D
47	73.23	33.72	1.8	374.899	C
48	73.1	33.66	15.4	267.953	D
49	73.28	33.58	3.8	376.249	C
50	73.18	33.56	9.7	398.759	C
51	73.27	33.69	2.1	377.065	C
52	73.14	33.75	111.1	269.266	D
53	73.12	33.69	3.5	526.63	C
54	73.12	33.69	24.4	553.736	C
55	73.07	33.74	19.6	365.741	C
56	72.84	33.67	31.8	431.88	C
57	72.91	33.68	10.2	258.096	D
58	73.17	33.78	27.5	375.902	C
59	73.08	33.69	93.9	264.307	D
60	73.2	33.55	96.2	327.802	D
61	73.12	33.54	90.2	385.9	C

(*continued*)

Table 2. Continued.

Site No.	Longitude (°)	Latitude (°)	Depth, H (m)	V_{S30} (m/s)	Site class, BCP (2007)
62	72.98	33.71	1.2	393.553	C
63	73.04	33.73	4.1	430.819	C
64	73.02	33.71	3.6	403.82	C
65	72.97	33.69	93.9	464.639	C
66	73.06	33.74	24.5	365.741	C
67	73.21	33.67	3.3	213.652	D
68	73.13	33.63	3.9	420.502	C
69	72.98	33.6	77.6	288.931	D
70	73.06	33.6	45.4	181.759	D
71	72.81	33.63	1.1	396.013	C
72	72.87	33.55	1.4	219.397	D
73	72.96	33.55	77.6	330.022	D
74	73.35	33.51	1.1	317.744	D
75	73.29	33.57	6.6	203.877	D
76	73.31	33.53	13	451.145	C
77	73.29	33.51	9.5	310.024	D
78	73.33	33.58	4.7	407.025	C
79	73.06	33.53	47.1	383.148	C
80	73.01	33.57	85.6	316.413	D
81	72.83	33.58	20.2	417.23	C
82	72.89	33.61	7.5	315.988	D
83	72.85	33.6	11.5	389.727	C
84	72.88	33.58	44.1	228.502	D
85	73	33.52	1.5	371.999	C

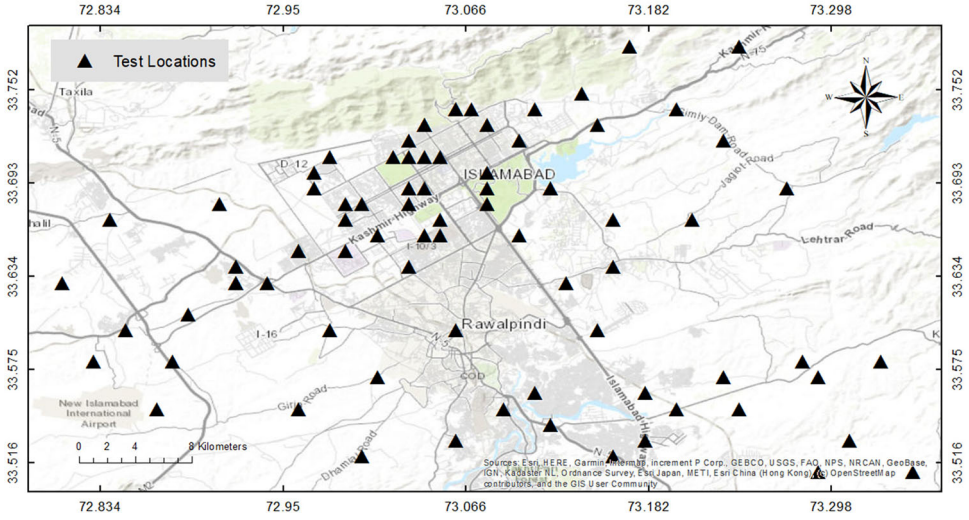

Figure 1. Location points for data acquisition in the Rawalpindi-Islamabad metropolitan area considered in this study.

$$V_{S30} = \frac{30}{\sum_{i=1}^{n} \frac{h_i}{V_{Si}}} \tag{8}$$

where h_i and V_{Si} are the soil layer thickness and shear wave velocity for layer i, respectively. V_{S30} of the site profiles range from 148 to 554 m/s. Only the profiles with depth up to 30 m are used. Figure 3 shows the distribution of V_S profiles among

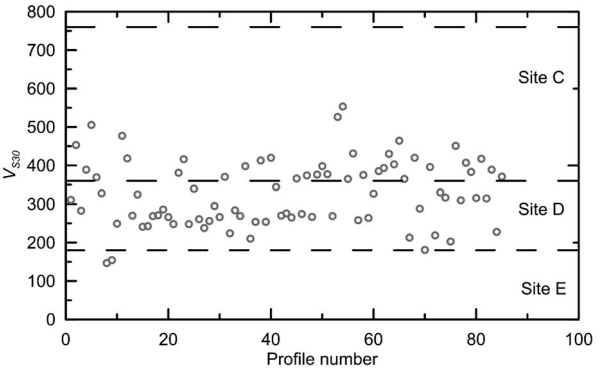

Figure 2. V_{S30} distribution of the 85 measured profiles as per BCP (2007) site classification system.

site class C, D and E according to BCP (2007). Mean V_S profile of each site class is also shown. It is demonstrated that there is no reversals observed in the measurements.

Before we begin to derive the correlation of V_{S30} with V_{SZ} at various shallow depths, it is necessary to analyze the proxies based V_{S30} estimation. These proxies include topographic slopes, geology, geomorphology, and/or hybrid approaches. In this study, slope and geology proxies were tested. Starting with the global-scale GMTED2010 digital elevation model (Danielson and Gesch 2011), geographic slope and elevations of borehole location. The resulting geographic slope values versus measurements of V_{S30} are shown in Figure 4. This figure demonstrates the topographic slope has a very weak correlation of $R^2 = 0.019$. Similarly, a very weak correlation of $R^2 = 0.002$ is observed by comparing the GMTED2010 digital elevation model-derived terrain elevation and the measured V_{S30}. The results are in line with Shafique et al. (2018). Table 3 provides a summary of the geology of the Islamabad-Rawalpindi region. This table contains information on geological formation in addition to the mean and median values of V_{S30} and BCP (2007) site classes. Additional information on the geology of this region may be obtained in the study of Khan et al. (2020). It has been intimated that the measured V_{S30} can only classify two sites (site classes C and D) within the restricted band of V_{S30} values. This may be due to the existence of a variety of geological formations as well as a little variation in V_{S30} values. It is also important to note that the estimation of V_{S30} cannot be strictly confined to the surficial geology since there is not a distinct transition in the values of V_{S30}.

3. Prediction of V_{S30} using shallow V_S profiles

In this section, the correlations of V_{S30} with V_{SZ} at various shallow depths are derived. In addition, the function development is explained in detail.

The correlations to predict V_{S30} at shallow depths require two variables: z and the corresponding V_{SZ}. Five representative depths of 5, 10, 15, 20 and 25 m are selected to derive the possible correlations between V_{SZ} (V_{S05}, V_{S10}, V_{S15}, V_{S20}, V_{S25}) and V_{S30}. These correlations are then generalized and can be used to calculate V_{S30} from any shallowest depth. Using the collected V_S profiles, the V_{SZ} values at the representative

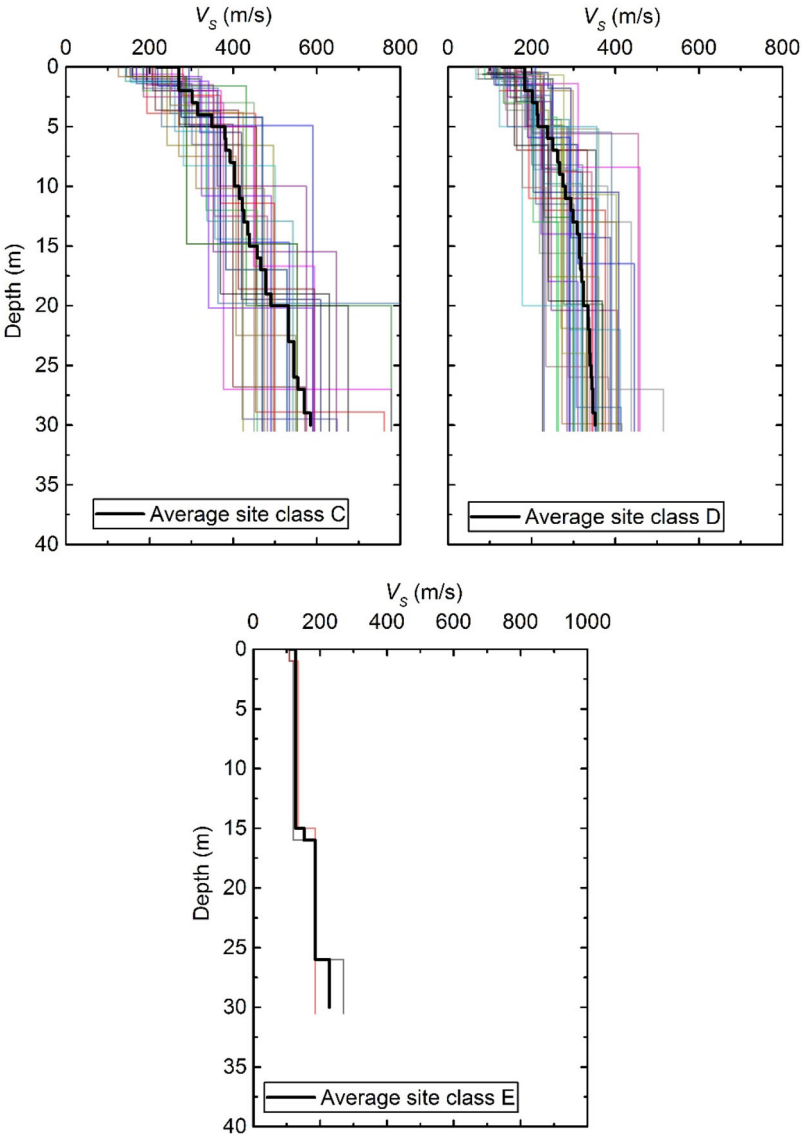

Figure 3. Measured V_S profiles categorized according to BCP (2007) into site classes: (a) C, (b) D, (c) E.

depths are calculated. Least squares linear regressions are performed to correlate V_{SZ} with V_{S30}. Figure 5 illustrates some examples of the correlations between V_{SZ} (V_{S10}, V_{S15}, V_{S20}, V_{S25}) and V_{S30}. It is demonstrated that the coefficient of determination (R^2) increases as the depths get closer to 30 m which confirms a stronger correlation of V_{SZ} with V_{S30} at higher depths. A linear trend is observed which is in line with the studies of B04 and S15. Table 4 summarizes the generic functional form proposed in this study along with the associated R^2 values. It should be noted that the R^2 values computed from the correlations in this study are slightly higher than the published studies, ranging from 0.70 to 0.998. This reveals that proposed functions fits the data

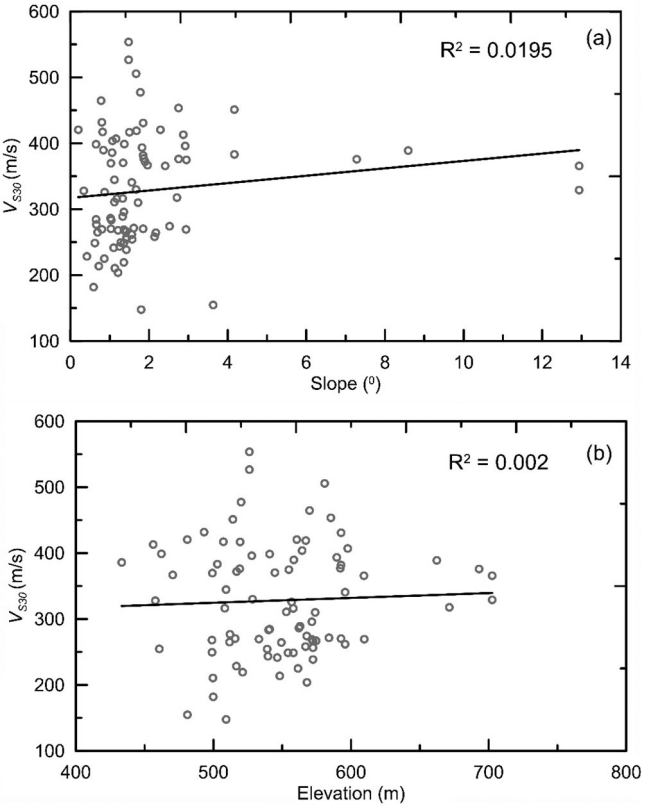

Figure 4. Correlation of measured Vs_{30} with the GMTED2010 digital elevation model (a) topographic slope, and (b) elevation.

well and follow the measurement trend. The functions proposed in this study are similar to S15, as defined in Eq. (2) but different than B04 and LEA15.

Figure 6 depicts the correlations between the five selected V_{SZ} and V_{S30}. At lower V_{S30} values ($V_{S30} < 200$ m/s), the predictions using V_{SZ} at all representative depths are demonstrated to converge. This indicates that the difference between V_{S30} and V_{SZ} is minimal at soft sites, whereas it increases as the sites become stiffer. In general, the overall trend of these correlations yields a slope that has a propensity to decrease as V_{sz} decreases. These slopes are then analyzed to develop a general function for estimating the V_{S30} from time-averaged shear wave velocity at any shallower depth. The coefficients of the representative V_{SZ} and V_{S30} correlations listed in Table 4 are illustrated in Figure 7 at corresponding depths. It is to worth mention here that the slopes of five selected V_{SZ} and V_{S30} relations are taken as coefficients for average V_S (C_s) and then nonlinear regression is performed with respect to z. Figure 7 reveals that Cs increases proportionally with z, $C_s = 0.67$ at z of 5 m and ultimately reaches unity at 30 m. C_S and z are strongly correlated and hence provide the basis for developing a generalized empirical correlation between V_{SZ} and V_{S30}. This trend is in line with the study of S15. The derived correlation is a modified version of the equation proposed in S15 and can be used to calculate V_{S30} at any shallow depth using the time-averaged shear wave velocity at depth. It is defined as follows:

Table 3. Comparison of local geology, mean and median V_{S30}, and site classification BCP (2007) (after Khan et al. 2020).

S. No.	Material type	Description	Number of measurements	Mean V_{S30} (m/s)	Median V_{S30} (m/s)	Site Class
1	Loose sediments	Fan alluvium	6	312	278	D
2	Loose sediments	Dissected windblown silt	21	279	266	D
3	Moderately strong rock	Limestone gravel conglomerate	4	304	324	D
4	Loose sediments	Flood-plain alluvium	1	399	399	C
5	Weak rock	Eroded, unconsolidated or very weakly consolidated mudstone, sandstone, and conglomerate	1	255	255	D
6	Weak rock	Undissected, unconsolidated or very weakly consolidated Undissected, unconsolidated or very weakly consolidated	3	344	376	C
7	Moderately strong rock	Limestone	5	387	382	C
8	Moderately strong rock	Interbedded sandstone and shale	8	418	404	C
9	Loose sediments	Undissected windblown silt	27	337	345	D
10	Loose sediments	Stream-channel alluvium	3	387	375	C
11	Loose sediments	Stream-terrace alluvium	4	285	273	D
12	Weak rock	Crystalline gravel conglomerate	2	284	284	D

$$V_{S30} = \frac{V_{SZ}}{C_s} \tag{9}$$

where C_S is defined as follows:

$$CS = 0.4643\ z^{0.2239} \tag{10}$$

Figure 8 compares V_{S30} estimated by the function proposed in this study with the predictions of V_{S30} by B04, S15, LEA15, WW15, and ZEA21 at z of 10, 15, 20, and 25 m. As explained in the introduction of this article, WW15 requires time-averaged shear wave velocity at two depths of the borehole, therefore, z_1 was set to 5 m because it was reported to result in a minimum error. For ZEA21, the M-Pt model developed in their study was used in this study because of its better performance, as reported in ZEA21. A comparative analysis revealed that the V_{S30} values predicted by B04 and ZEA21 results in a close match with the V_{S30} values estimated in this study. This trend is consistent for all the representative depths considered. S15 results in the highest prediction of V_{S30} among all the studies presented here. LEA15 correlation over predicts for $V_{S30} < 250$ m/s and under predicts otherwise. This demonstrates that the site characteristics of the Rawalpindi–Islamabad region differ from those of Karachi. Hence, the correlation proposed by LEA15 cannot be possibly applied to the region under study. It is to note that all the correlations presented here results in a straight line fit with the exception of the LEA15 model. The empirical model derived by B04 and ZEA21 from a large number of sites are shown to produce surprisingly favorable fits. However, it should be noted that WW15 and ZEA21 requires V_S measurements up to 30 m to calculate V_{S30} from V_{SZ}, which practically reduces the effectiveness of these correlations. Although the B04 and ZEA21 models follow the trend

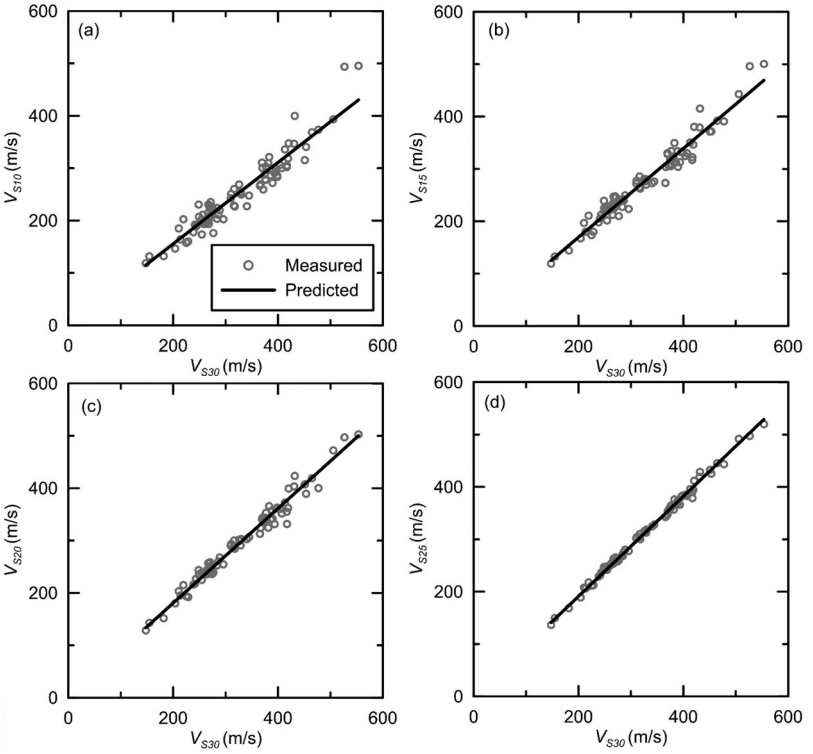

Figure 5. Correlations between measured V_{S30} and: (a) V_{S10}, (b) V_{S15}, (c) V_{S20}, (d) V_{S25}, along with the predictions using proposed Eq. (9).

Table 4. Correlations between V_{S30} and V_{SZ} at five representative depths.

Depth (m)	Function	R^2
5	$V_{S05} = 0.6696\, V_{S30}$	0.706
10	$V_{S10} = 0.7773\, V_{S30}$	0.839
15	$V_{S15} = 0.8472\, V_{S30}$	0.932
20	$V_{S20} = 0.9033\, V_{S30}$	0.998
25	$V_{S25} = 0.9553\, V_{S30}$	0.999

of measured data points, the proposed model exhibits lower residuals as compared to both the models. Figure 9 illustrates the variation of Root Mean Square Error (RMSE) with depth from all the correlations. For each depth z, the V_{S30} was predicted from Vsz and the RMSE was defined as follows:

$$\mathrm{RMSE} = \sqrt{\frac{\sum_{i=1}^{85}(\mathrm{Predicted}_i - \mathrm{Measured}_i)^2}{85}} \tag{11}$$

RMSE reduces for all the correlations as the depths approach 30 m. It is demonstrated that S15 results in the highest RMSE across all depths. RMSE from WW15 and LEA15 is comparable for $z \geq 10$ m. RMSE from the proposed correlations is considerably lower at $z = 5$ m, whereas, it is comparable with B04 and ZEA21 for

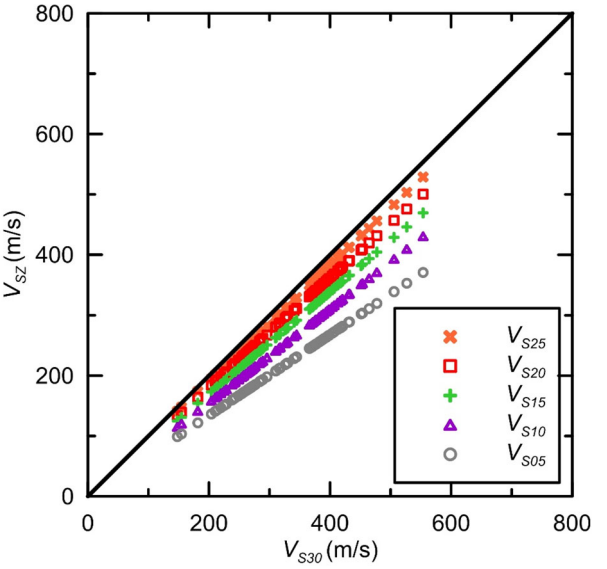

Figure 6. Prediction of V_{S30} from V_{sz} (Vs_{05}, Vs_{10}, Vs_{15}, Vs_{20}, Vs_{25}) using the proposed correlation in Eq. (9).

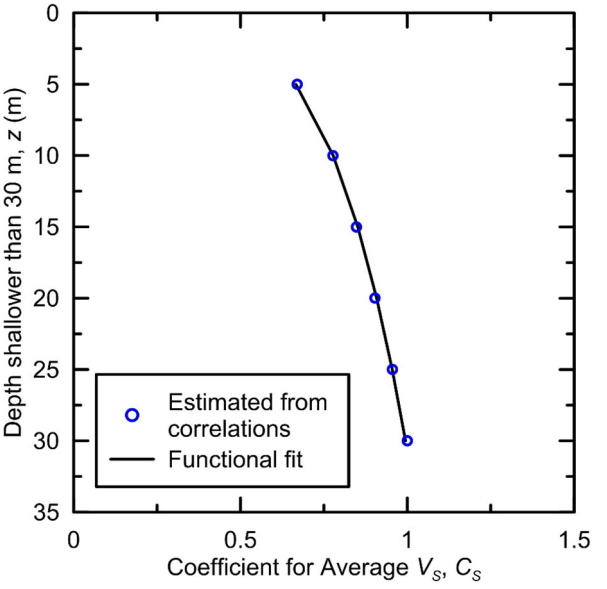

Figure 7. Correlation between depth (z) less than 30 m and coefficient for average V_S (Cs) proposed in Eq. (10).

$z \geq 10$ m. However, the RMSE produced by this study is lowest among all the studies under investigation across all depths.

The efficacy of the proposed method is assessed by using the ratio of estimated V_{S30} and measured V_{S30} (V_{S30} predicted/V_{S30} measured). Figure 10 plots the V_{S30} ratio for all the test locations at the depths of 5, 10, 15, 20, and 25 m. The largest dispersion is observed for the depth of 5 m but the error is not significant. A maximum standard

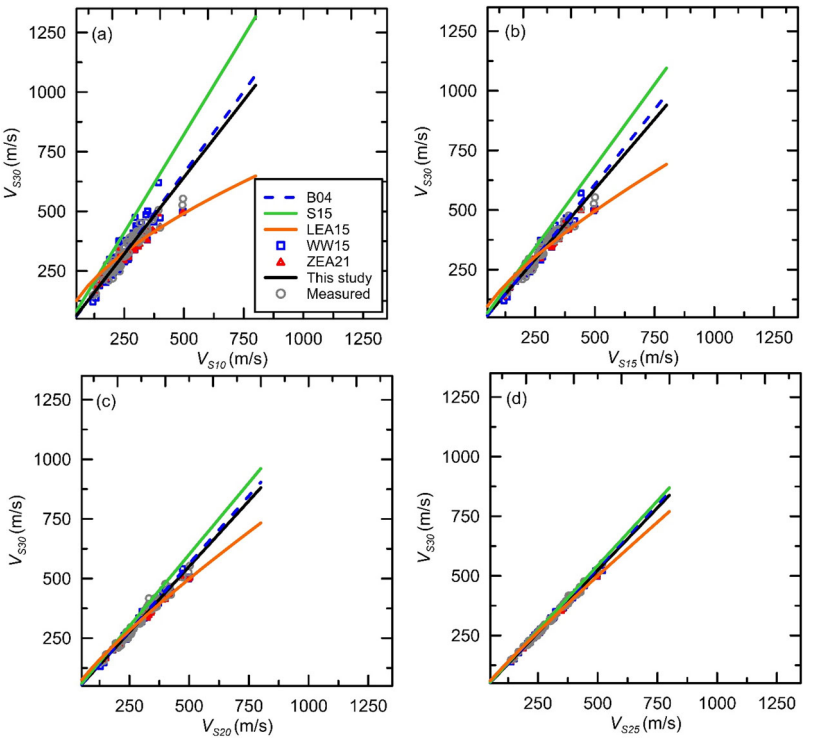

Figure 8. Comparison of the V_{S30} predictions in this study with the selected published studies in the literature at depths: (a) 10, (b) 15, (c) 20, and (d) 25 m.

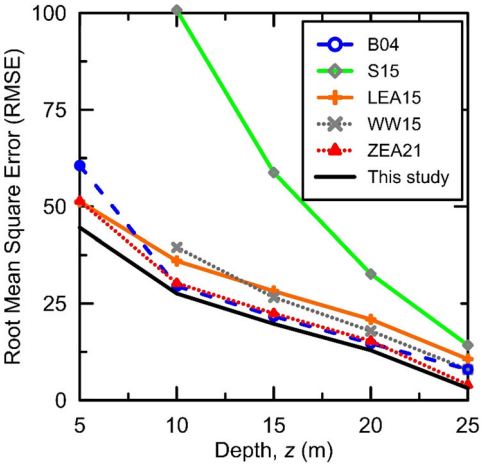

Figure 9. Variation of RMSE with depth for the correlations under investigation.

deviation of 0.12 was calculated among the ratios at all the depths which demonstrates inconsiderable error in the predictions from the proposed correlations. The dispersion decreases as the depth increases. At the depths of 20 and 25 m, most of the points fall on the unity line, demonstrating the efficiency of the proposed method.

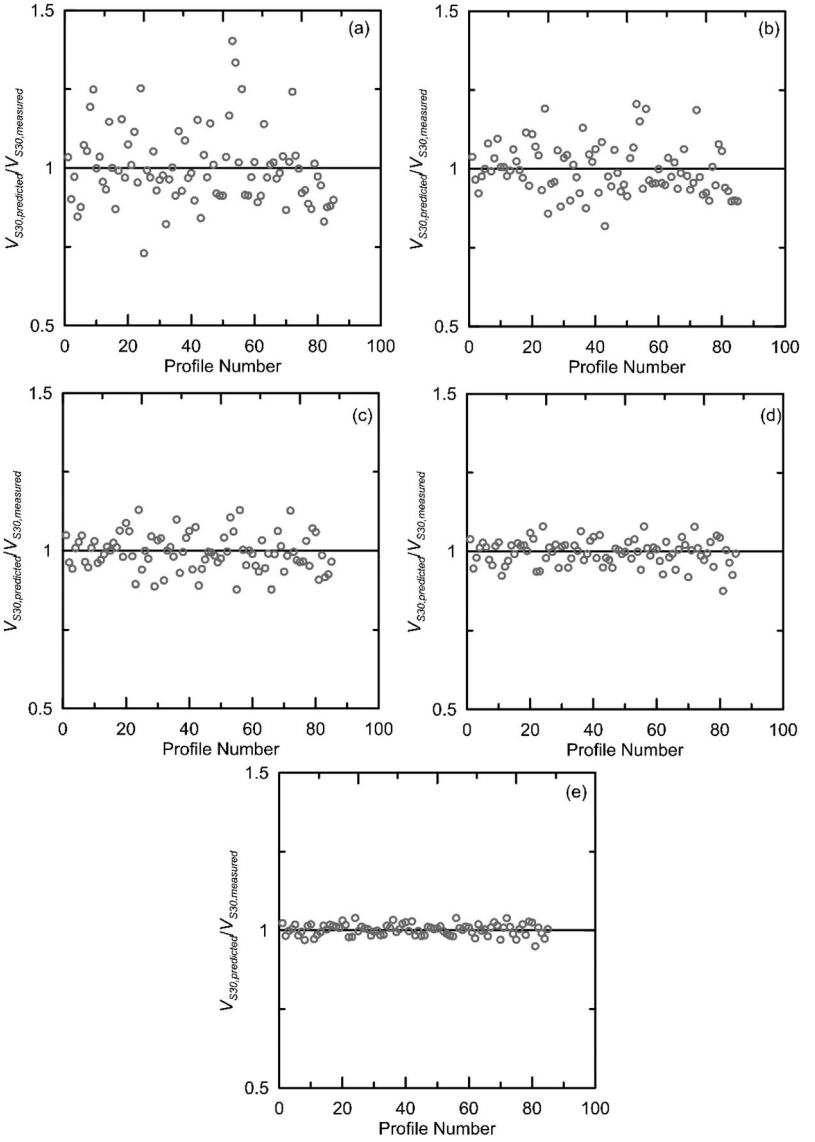

Figure 10. Variation of predicted and measured V_{S30} ratio at all the test locations from: (a) V_{S10}, (b) V_{S15}, (c) V_{S20}, and (d) V_{S25}.

4. Prediction of V_S profiles from shallow depths to 30 m

As mentioned earlier, V_S profile up to the bedrock or up to 30 m is needed for quantification of ground response under an earthquake loading. In this section, a method to generate the V_S profile up to 30 m for the Rawalpindi–Islamabad is developed. A mean V_S profile from all the 85 V_S profiles used in this study is developed at 1 m intervals up to 30 m. A second order polynomial function similar to that used in S15 is then fitted to the mean V_S profile. The following second order polynomial function is proposed to provide V_S at any depth up to 30 m, because it was reported that this function provides sufficient fit to the data (Boore et al. 2011):

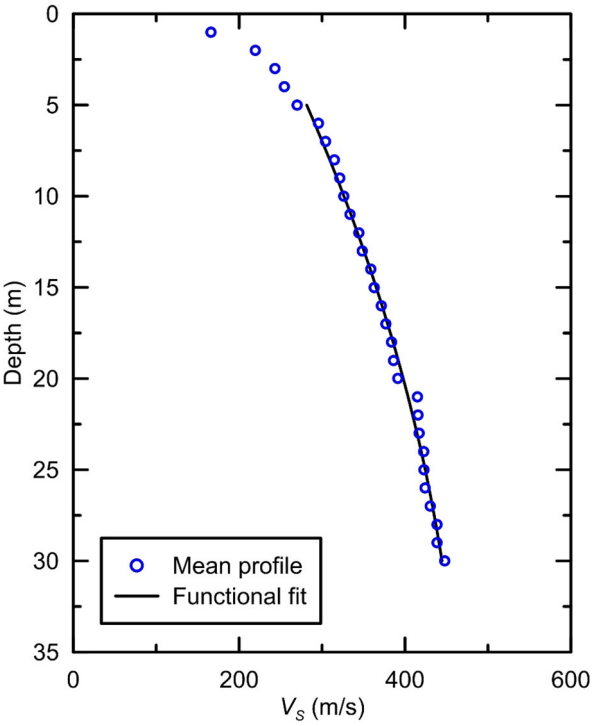

Figure 11. Polynomial function proposed in Eq. (13) fitted to the mean shear wave velocity profile for depths 5–30 m.

$$V_S = -0.124\ z_c^{\,2} + 10.866\ z_c + 230.1902 \tag{12}$$

The fitted curve along with the mean V_S profile data points is shown in Figure 11. The function is correlated from depths from 5 to 30 m.

To generalize the expression for acquiring V_S from any shallow depth for any shallow profile, the expression should describe the final measured depth and V_S at that depth. The function is defined as follows:

$$V_S\ = -0.124\ z_c^{\,2} + 10.866\ z_c - V_S\ (z_c) \tag{13}$$

$V_S\ (z_c)$ is defined as follows:

$$V_S\ (z_c) = -0.124\ z_{c(cut\ \ off)}^{\ \ 2} + 10.866\ z_{c(cut\ \ off)} - V_{S(cut\ \ off)} \tag{14}$$

Figure 12 illustrates a representative profile measured from field up to 15 m. The function shown in Eq. (13) is used to construct the profile from 15 m onwards. V_S profile assuming constant velocity from the shallowest available depth up to 30 m is also shown along with the representative measured profile. The proposed expression is demonstrated to effectively extrapolate the profile up to 30 m. The percentage difference between the extrapolated and the measured profile ranges from 2% at 15 m to 9% at 30 m. It is worth mentioning that the use of extrapolated function provides

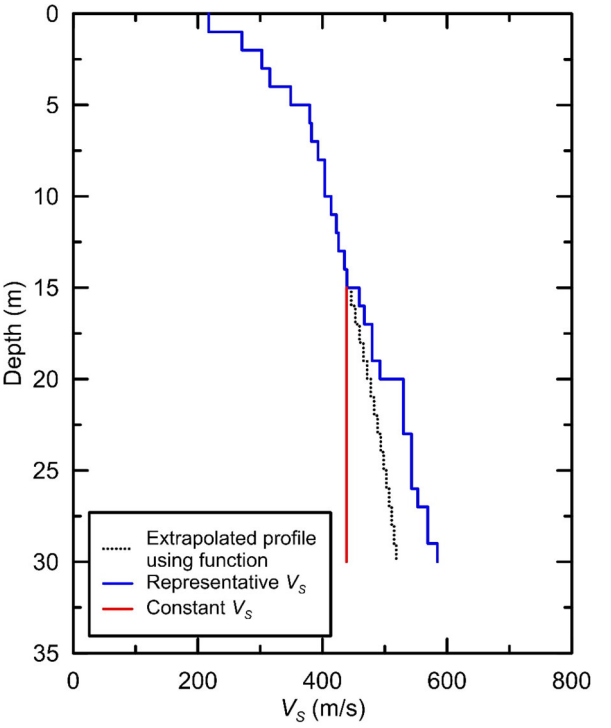

Figure 12. An example of extrapolation of V_S profile using the function proposed in Eq. (13).

much better estimates than assuming the constant V_S profile from the point where the field testing is discontinued and up to 30 m. It should be noted that the uncertainties were not accounted for as this was the first attempt for developing the V_S profile up to 30 m from shallow profiles in Pakistan. It should also be noted that the developed function is independent of site class and did not account for all possible soil types or soil conditions. These issues should be considered in the future studies.

5. Conclusions

The evaluation of ground motion characteristics and site classification requires V_{S30} estimation. In this study, a total of 85 V_S profiles measured up to 30 m from Rawalpindi-Islamabad region are utilized to develop the V_{S30} prediction function from shallow V_S profiles. Additionally, a function for extrapolating V_S profile from shallow depths to 30 m is also developed. Moreover, the topography and geology of the region are also taken into consideration for a possible correlation with V_{S30}. It is revealed that topographic slope and geology proxies show a weak with low confidence relationship with measured data. As a result, the region-specific extrapolation method is developed.

The V_{S30} values of the available profiles are correlated with corresponding time-averaged shear wave velocity at five representative depths of 5, 10, 15, 20 and 25 m. Least squares linear regression was performed and the functions are demonstrated to

have a high coefficient of determination. These correlations yield a generalized function to determine the V_{S30} from the time-averaged shear wave velocity at shallower depths. A comparative analysis of the proposed procedure is carried out with the published methods. It reveals that the V_{S30} predicted by the function used in this study results in a close match with those in the western United States and China.

We also analyze the performance of five existing functions and proposed relation with measured data using RMSE. The empirical relation developed in this study outperforms all five models for all depths. The S15 shows the highest RMSE throughout the depths whereas ZEA21 exhibits low errors among other functions. B04 has comparable performances with ZEA21 at all depths except $z < 10$ m. LEA15 and WW15 show subpar performance.

To extrapolate the V_S profile from shallower depths to 30 m, average V_S profile of all the sites in this study is used. A quadratic function is used to fit the representative mean V_S curve. This function is then utilized to propose a generalize function for extrapolating V_S from shallow depths. A comparison with the constant V_S extrapolation method reveals that the V_S extrapolated using the function proposed in this study results in a realistic V_S profile. In general, the empirical function developed for V_{S30}, and the V_S extrapolation method may be used to quantify seismic hazard risk in the region.

Disclosure statement

No potential conflict of interest was reported by the authors.

ORCID

Duhee Park http://orcid.org/0000-0002-0180-2668

Data availability statement

Shear wave velocity dataset analyzed during the current study was collected using HVSR testing procedures by Dr. Sarfraz Khan, who is also the co-author of this manuscript. It is available from the corresponding author upon request and is also available in Khan et al. (2020).

References

Aaqib M, Park D, Adeel MB, Hashash YM, Ilhan O. 2021. Simulation-based site amplification model for shallow bedrock sites in Korea. Earthq Spectra. 37(3):1900–1930.

Aaqib M, Park D, Kim H, Adeel MB, Nizamani ZA. 2020. Evaluation of the influence of shear strength correction through a comparative study of nonlinear site response models. J Korean Geotechn Soc. 36(12):77–86.

Aaqib M, Park D, Lee Y-G, Pervaiz U. 2022. Development of site classification system and seismic site coefficients for Korea. J Earthquake Eng. 26(16):8257–8279.

Aaqib M, Sadiq S, Park D, Hashash YM, Pehlivan M. 2018. Importance of implied strength correction for 1D site response at shallow sites at a moderate to low seismicity region. In Geotechnical Earthquake Engineering and Soil Dynamics V. American Society of Civil Engineers, Reston, VA; p. 445–453.

Adeel MB, Aaqib M, Pervaiz U, Ur Rehman J, Park D. 2022. Numerical response of pile foundations in granular soils subjected to lateral load. Geomech Eng. 28(1):11–23.
Adeel MB, Jan MA, Aaqib M, Park D. 2020. Development of simulation based p-multipliers for laterally loaded pile groups in granular soil using 3D nonlinear finite element model. Appl Sci, 11(1):26
Allen TI, Wald DJ. 2009. On the use of high-resolution topographic data as a proxy for seismic site conditions (VS 30). Bull Seismol Soc Am. 99(2A):935–943.
Anderson JG, Lee Y, Zeng Y, Day S. 1996. Control of strong motion by the upper 30 meters. Bull Seismol Soc Am. 86(6):1749–1759.
BCP 2007. Building Codes of Pakistan Seismic Provisions Government of Islamic republic of Pakistan Ministry of Housing and Works. Islamabad.
Bhusal B, Aaqib M, Paudel S, Parajuli HRJG. 2022. Site specific seismic hazard analysis of monumental site Dharahara, Kathmandu, Nepal. Geomatics Nat Hazards Risk. 13(1): 2674–2696.
Bindi D, Luzi L, Pacor F, Franceschina G, Castro R. 2006. Ground-motion predictions from empirical attenuation relationships versus recorded data: the case of the 1997–1998 Umbria-Marche, central Italy, strong-motion data set. Bull Seismol Soc Am. 96(3):984–1002.
Boore DM. 2004. Estimating Vs(30)(or NEHRP site classes) from shallow velocity models (depths< 30 m). Bull Seismol Soc Am. 94(2):591–597.
Boore DM, Joyner WB, Fumal TE. 1997. Equations for estimating horizontal response spectra and peak acceleration from western North American earthquakes: a summary of recent work. Seismol Res Lett. 68(1):128–153.
Boore DM, Thompson EM, Cadet H. 2011. Regional correlations of VS 30 and velocities averaged over depths less than and greater than 30 meters. Bull Seismol Soc Am. 101(6): 3046–3059.
Cadet H, Duval A-M. 2009. A shear wave velocity study based on the KiK-net borehole data: a short note. Seismol Res Lett. 80(3):440–445.
Campbell KW, Bozorgnia Y. 2008. NGA ground motion model for the geometric mean horizontal component of PGA, PGV, PGD and 5% damped linear elastic response spectra for periods ranging from 0.01 to 10 s. Earthq Spectra. 24(1):139–171.
Chiou BSJ, Youngs RR. 2014. Update of the Chiou and Youngs NGA model for the average horizontal component of peak ground motion and response spectra. Earthq Spectra. 30(3): 1117–1153.
Council BSS 1997. NEHRP recommended provisions for seismic regulations for new buildings and other structures.
Danielson JJ, Gesch DB. 2011. Global multi-resolution terrain elevation data 2010 (GMTED2010). Washington, DC, USA: US Department of the Interior, US Geological Survey.
Durrani AJ, Elnashai AS, Hashash Y, Kim SJ, Masud A. 2005. The Kashmir earthquake of October 8, 2005: a quick look report. MAE Center CD Release 05–04.
Pokhrel RM, Gilder CE, Vardanega PJ, De Luca F, Werner MJ, Maskey PN. 2019. April. Estimation of VS30 by HVSR method at a site in the Kathmandu Valley, Nepal. In 2nd international conference on earthquake engineering and post disaster reconstruction planning (ICEE-PDRP).
Gaha TB, Bhusal B, Paudel S, Saru S. 2022. Investigation of ground response analysis for Kathmandu valley: a case study of Gorkha earthquake. Arab. J. Geosci, 15(15):1–14.
Gansser A. 1964. Geology of the Himalayas. New York: Interscience.
Gee E, Gee D. 1989. Overview of the geology and structure of the Salt Range, with observations on related areas of northern Pakistan. Geological Society of America special paper. 232:p. 95–112.
Harmon J, Hashash YMA, Stewart JP, Rathje EM, Campbell KW, Silva WJ, Ilhan O. 2019. Site Amplification Functions for Central and Eastern North America – Part II: modular Simulation-Based Models. Earthquake Spectra. 35(2):815–847.
ICC I 2015. International Building Code, Washington, DC.

Khan S, Khan MA. 2018. Seismic Microzonation of Islamabad–Rawalpindi Metropolitan Area, Pakistan. Pure Appl Geophys. 175(1):149–164.
Khan S, Waseem M and Khan MA. 2021. A Seismic hazard map based on geology and shear-wave velocity in Rawalpindi–Islamabad, Pakistan. Acta Geologica Sinica-English Edition. 95(2):659–673.
Kramer SL. 1996. Geotechnical earthquake engineering. Noida, India: Pearson Education.
Kuo C-H, Wen K-L, Hsieh H-H, Chang T-M, Lin C-M, Chen C-T. 2011. Evaluating empirical regression equations for Vs and estimating Vs30 in northeastern Taiwan. Soil Dyn Earthq Eng. 31(3):431–439.
Lee SHH. 1990. Regression models of shear wave velocities in Taipei basin. J Chin Inst Eng. 13(5):519–532.
Li X, Jing B, Liu C, Yin J. 2019. Site classification method based on geomorphological and geological characteristics and its application in China. Bull Seismol Soc Am. 109(5):1843–1854.
Lodi S, Kumar M, Samad M, Wasim A. 2015. Predictive relationship for estimation of V s30 using shallow bore logs for Karachi. Geotech Geol Eng. 33(3):559–573.
Mahmood K, Rehman Zia-ur, Farooq K, Memon SA. 2016. One dimensional equivalent linear ground response analysis—a case study of collapsed Margalla Tower in Islamabad during 2005 Muzaffarabad Earthquake. J Appl Geophys. 130:110–117.
Manandhar S, Cho H-I, Kim D-S. 2018. Site classification system and site coefficients for shallow bedrock sites in Korea. J Earthquake Eng. 22(7):1259–1284.
Midorikawa S, Nogi Y. 2015. Estimation of VS30 from shallow velocity profile. J Jpn Assoc Earthq Eng. (2):91–96.
Monalisa, Khwaja AA, Jan MQ. 2007. Seismic hazard assessment of the NW Himalayan fold-and-thrust belt, Pakistan, using probabilistic approach. Journal of Earthquake Engineering. 11(2):257–301.
Nguyen V-Q, Aaqib M, Nguyen D-D, Luat N-V, Park D. 2020. A site-specific response analysis: a case study in Hanoi, Vietnam. Applied Sciences. 10(11):3972.
Nizamani ZA, Park D. 2021. Testing ground-motion prediction equations against moderate magnitude earthquake data recorded in Korea. Bull Seismol Soc Am. 111(1):321–338.
Sadiq S, Muhammad A, Mandokhail SUJ, Rehman M-U, Mehtab A, Muhammad N, Adeel MB. 2021. Evaluation of Site Amplification Factors for Shallow Rock Sites of Islamabad, Kuwait J Sci. 48(2).
Seyhan E, Stewart JP. 2014. Semi-empirical nonlinear site amplification from NGA-West2 data and simulations. Earthq Spectra. 30(3):1241–1256.
Shafique M, Hussain ML, Asif Khan M, van der Meijde M, Khan S. 2018. Geology as a proxy for Vs30-based seismic site characterization, a case study of northern Pakistan. Arab J Geosci. 11(12):1–12.
Sun C-G. 2015. Determination of mean shear wave velocity to 30 m depth for site classification using shallow depth shear wave velocity profile in Korea. Soil Dyn Earthq Eng. 73: 17–28.
Sun C-G, Kim D-S, Chung C-K. 2005. Geologic site conditions and site coefficients for estimating earthquake ground motions in the inland areas of Korea. Eng Geol. 81(4):446–469.
Thompson EM, Baise LG, Kayen RE, Tanaka Y, Tanaka H. 2010. A geostatistical approach to mapping site response spectral amplifications. Eng Geol. 114(3–4):330–342.
Tran N-L, Aaqib M, Nguyen B-P, Nguyen D-D, Tran V-L, Nguyen V-Q. 2021. Evaluation of seismic site amplification using 1D site response analyses at Ba Dinh Square Area, Vietnam. Adv Civ Eng. 2021:1–11.
Wald DJ, Allen TI. 2007. Topographic slope as a proxy for seismic site conditions and amplification. Bull Seismol Soc Am. 97(5):1379–1395.
Wang HY, Wang SY, 2015. A new method for estimating VS (30) from a shallow shear-wave velocity profile (depth< 30 m). Bull Seismol Soc Am. 105(3):1359–1370.
Wills C, Clahan K. 2006. Developing a map of geologically defined site-condition categories for California. Bull Seismol Soc Am. 96(4A):1483–1501.

Wills C, Gutierrez C, Perez F, Branum D. 2015. A next generation VS30 map for California based on geology and topography. Geol Topogr. 105(6):3083–3091.

Wills C, Petersen M, Bryant W, Reichle M, Saucedo G, Tan S, Taylor G, JJBotSSoA T. 2000. A site-conditions map for California based on geology and shear-wave velocity. Bull Seismol Soc Am. 90(6B):S187–S208.

Xie J, Zimmaro P, Li X, Wen Z, Song Y. 2016. VS 30 empirical prediction relationships based on a new soil-profile database for the Beijing plain area, China. Bull Seismol Soc Am.106(6):2843–2854.

Yaghmaei-Sabegh S, Rupakhety R. 2020. A new method of seismic site classification using HVSR curves: case study of the 12 November 2017 Mw 7.3 Ezgeleh earthquake in Iran. Eng Geol. 270:105574.

Yong A, Hough SE, Abrams MJ, Cox HM, Wills CJ, Simila GW. 2008. Site characterization using integrated imaging analysis methods on satellite data of the Islamabad, Pakistan, region. Bull Seismol Soc Am. 98(6):2679–2693.

Zhou J, Li X, Dai Z, Chen, K. 2021. Parametrical Model for Estimating VS30 from shallow borehole profiles using a database for China. Bull Seismol Soc Am. 111(3):1199–1220.